Inorganic Chemistry Communications 13 (2010) 273–277

Contents lists available at ScienceDirect

Inorganic Chemistry Communications

journal homepage: www.elsevier.com/locate/inoche

# Ru(II)–CO complexes of thioarylazoimidazoles: Syntheses, structures, spectroscopy and DFT calculation

T.K. Mondal [a], P. Raghavaiah [b], A.K. Patra [c], C. Sinha [a,*]

[a] Department of Chemistry, Inorganic Chemistry Section, Jadavpur University, Kolkata 700 032, India
[b] School of Chemistry, National Single Crystal X-ray Diffractometer Facility, University of Hyderabad, Hyderabad 500 046, India
[c] Indian Institute of Science, Bangalore 560 012, India

ARTICLE INFO

*Article history:*
Received 23 October 2009
Accepted 1 December 2009
Available online 5 December 2009

*Keywords:*
Ruthenium-carbonyl
Thioarylazoimidazoles
X-ray structure
Electrochemistry
DFT calculation

ABSTRACT

The complexes, *cis*-(CO)-*trans*-(Cl)-[Ru(SRaaiNR)$(CO)_2Cl_2$] (**2**) and *trans*-(Cl)-[Ru(SRaaiNR)$(CO)Cl_2$] (**3**) (SRaaiNR = 1-alkyl-2-{(*o*-thioalkyl)phenylazo}imidazoles; R = Me (**1a**) and Et (**1b**)) have been synthesized and characterized. The structural confirmation is achieved by single crystal X-ray structure determinations. The complexes show Ru(III)/Ru(II) couple and ligand reductions. Electronic structure and spectral properties of the complexes have been explained with the DFT and TDDFT calculation.



The coordination chemistry of ruthenium with pyridine and its derivatives is one of the most studied areas because of catalytic, redox, photoreactivity, biological and supramolecular properties of the complexes. Small variation in the coordination environment around ruthenium by changing donor centre, ligand structure and chelate ring size play a key role in altering the properties of the complexes [1,2]. The synthesis of new ligands in the framework of diimine group (–N=C–C=N–) [3] or to design conjugated system isoelectronic to diimine function such as azoimine, (–N=N–C=N–) [4] are of interest in the recent years. The attachment of arylazo (Ar–N=N–) group at *ortho*-position to a five- or six-membered N-heterocycle has synthesized azoimine function and have been used to explore the chemistry of transition [4,5] and non-transition metals [6–8]. Recently we have synthesized 1-alkyl-2-{(*o*-thioalkyl)phenylazo}imidazole (SRaaiNR) [9], a tridentate N(imidazole), N(azo) and S(thioether) ligand. This work is concerned with the syntheses, crystal structures, redox properties and correlation of spectral and electrochemical properties of a new series of ruthenium(II) carbonyl complexes of SRaaiNR. The spectral and redox properties are correlated with DFT and TDDFT computed results.

The syntheses of ligands are reported elsewhere [9]. The ligands SMeaaiNMe (**1a**) (1-methyl-2-{(*o*-thiomethyl)phenylazo}imidazole) and SEtaaiNEt (**1b**) (1-ethyl-2-{(*o*-thioethyl)phenylazo}imidazole react with $[Ru(CO)_2Cl_2]_n$ in 1:1 molar ratio in ethanol [10] under $N_2$ environment to afford hexa-coordinated red colored complexes *cis*-(CO)-*trans*-(Cl)-[Ru(SMeaaiNMe)$(CO)_2Cl_2$] (**2a**) and *cis*-(CO)-*trans*-(Cl)-[Ru(SEtaaiNEt)$(CO)_2Cl_2$] (**2a**), respectively (Scheme 1). The green colored complexes *trans*-(Cl)-[Ru(SRaaiNR)$(CO)Cl_2$] (**3a** and **3b**) have been synthesized from the similar reaction in acetonitrile in presence of excess $Me_3NO$ [11]. The complexes have been characterized by elemental analyses, $^1$H NMR, IR and UV–Vis spectroscopy together with single X-ray crystal structures of **2a** (Fig. 1a) and **3b** (Fig. 1b). Although S-centres in the ligand are susceptible to $O_2$ (in air) to produce sulfoxides/sulfones [12] but no such oxidation is observed in this reaction. Complex **2a** shows two equally intense ν(CO) bands at 2004 and 2066 $cm^{-1}$ ($\nu_{theo}$ = 2023 and 2072 $cm^{-1}$ for **2a**, calculated from optimized geometry of the compound using DFT computation technique); **2b** shows ν(CO) at 1998 and 2062 $cm^{-1}$ that suggests the presence of two carbonyl groups *cis* to each other. The spectra of **3a** and **3b** show only one strong stretching at 1995 and 1991 $cm^{-1}$, respectively corresponding to single ν(CO) ($\nu_{theo}$ = 2015 $cm^{-1}$ for **3b**). Other significant peaks appear at 1544–1555 $cm^{-1}$ and at 1370–1395 $cm^{-1}$ those correspond to *ν*(C=N) and *ν*(N=N), respectively. The azo (–N=N–) stretching is significantly shifted to lower frequency region compared to free ligand value (1400–1410 $cm^{-1}$) [9] which supports efficient back-donation, $d\pi(Ru^{II}) \rightarrow \pi^*(N{=}N)$. The electronic spectra of **2** show intense band at 495–500 nm and the complexes **3** exhibit transition at 590–595 nm along with weak band at 790–810 nm. Azoimidazoles are susceptible to light both at free and coordinated state in Hg(II), Cd(II) and Pd(II) complexes and undergo *trans*-to-*cis* photoisomerisation upon light irradiation [13]. Ruthenium(II) complexes are silent to photoisomerisation. There may be several reasons.

* Corresponding author. Fax: +91 033 2413 7121.
*E-mail address:* c_r_sinha@yahoo.com (C. Sinha).

1387-7003/$ - see front matter © 2009 Elsevier B.V. All rights reserved.
doi:10.1016/j.inoche.2009.12.001

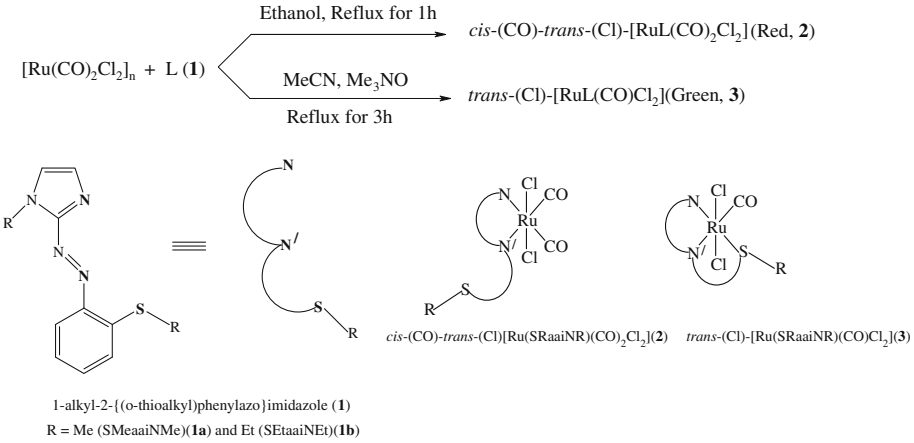


**Scheme 1.**

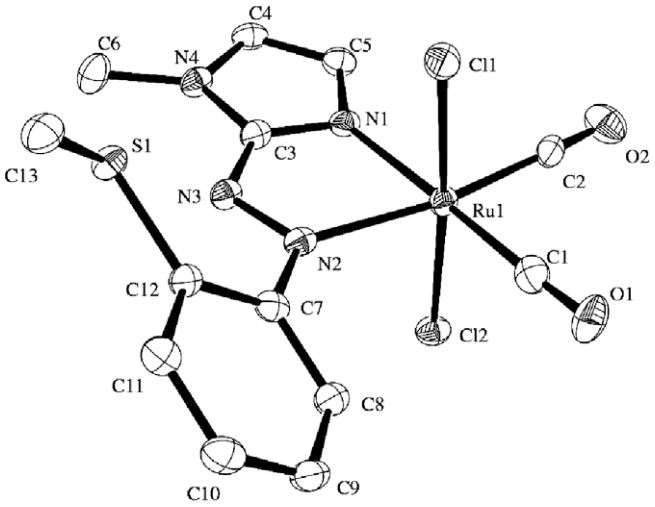


**Fig. 1a.** ORTEP structure of **2a** (35% probability). Hydrogen atoms have been omitted for clearity. Selected bond lengths (Å) and angles (°): Ru1–C1 1.888(3), Ru1–C2 1.909(3), Ru1–N1 2.102(2), Ru1–N2 2.146(2), Ru1–Cl1 2.3785(2), Ru1–Cl2 2.3959(6), O1–C1 1.127(4), O2–C2 1.090(3), N1–N2 1.285(3), N1–Ru1–N2 75.73(8), C1–Ru1–C2 90.91(11), Cl1–Ru1–Cl2 175.69(2).

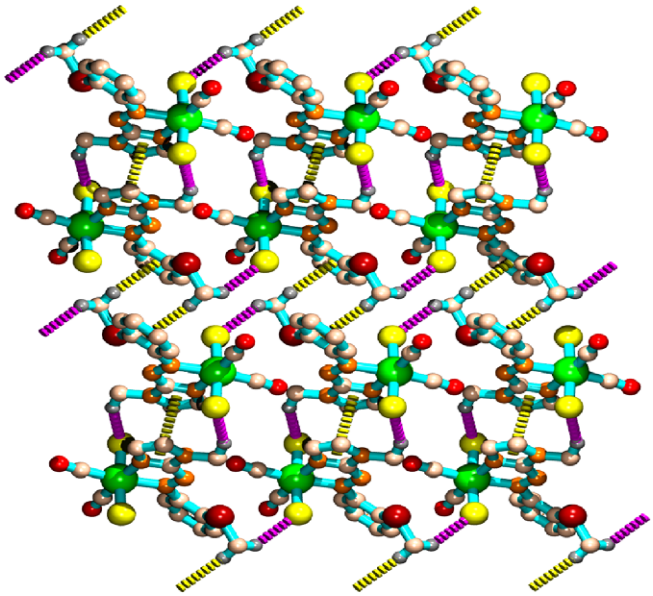

**Fig. 1b.** The 2D sheet (bc plane) through π–π, C–H···π and C–H···Cl hydrogen bonding in **2a**.

Ligand is chelated to Ru(II) and X-ray structure determination shows that Ru–N(azo) bond length is shorter than Ru–N(imidazole) distances. This has also prompted charge flow $d\pi(Ru) \rightarrow \pi^*$(azo) which synergistically enhances Ru–N(azo) bond strength. This structural rigidity may resist photoisomerisation. Besides, the energy transfer from ($\pi$–$\pi^*$) to MLCT state may cause very fast bleaching [14].

The crystal structure of **2a** (Fig. 1) shows distorted octahedral geometry with $RuCl_2C_2N_2$ coordination where SMeaaiNMe (**1a**) acts as bidentate N(imidazole), N(azo) chelator and thioether-S remains free and conformationally away from metal centre. Some general features in the molecule are: chelating ligand; two *cis*-CO constitute square plane, $Ru(C)_2(N, N)$ (C is donor centre of CO) while two *trans*-Cl are nearly perpendicular to this plane (∠Cl(1)–Ru(1)–Cl(2), 175.69(2)°. The chelate ring dimension (∠N(2)–Ru(1)–N(1), 75.73(8)°) is comparable with those of other structurally characterized azoimine chelated molecules [4,15–17]. The Ru–N(azo), [Ru(1)–N(2), 2.146(2) Å], is longer than Ru–N(imidazole) [Ru(1)–N(1), 2.102(2) Å]. In general, the Ru–N(azo) bond length is shorter than Ru–N(imidazole) bond which is mainly due to back-donation, $d\pi(Ru) \rightarrow \pi^*$(N=N), to azoimine ligand [4,17]. Two strongly π-acidic CO at cisoid conformation polarize Ru–N bonds and hence, Ru–N(azo) suffers considerably more room for exocyclic N(azo) than N(imidazole) [18]. Thus the van der Waals repulsion will be greater in N(azo) than N(imidazole). This may be the reason to reduce backbonding efficiency and the reversal of bond dimensions. The N=N bond length is 1.285(3) Å and is longer than free ligand azo distance (1.252(1) Å) [19] which supports back bonding conjecture. Intermolecular hydrogen bond between one of the coordinated Cl and H of one N–$CH_3$ group of adjacent molecule has generated dimer. The presence of C–H–π and π–π interactions between two adjacent imidazole rings generate supramolecular network (Fig. 1b).

In **3b**, 1-methyl-2-{(*o*-thioethyl)phenylazo}imidazole acts tridentate NN′S ligand and CO constitutes distorted square plane, Ru(C)(N, N, S) (C is donor centre of CO) and the two *trans*-Cl are nearly perpendicular to this plane (∠Cl(1)–Ru(1)–Cl(2), 176.38(2)° (Fig. 2). The chelate ring dimensions are ∠N(1)–Ru(1)–N(3): 76.65(7)° and ∠N(1)–Ru(1)–S(1), 84.43(5)°. In **2a** the azo ligand acts as bidentate N, N chelator, removal of CO may decrease the hardness of Ru and may prefer to bind thioether-S. This may enhance the backbonding efficiency in **3b**. The immediate

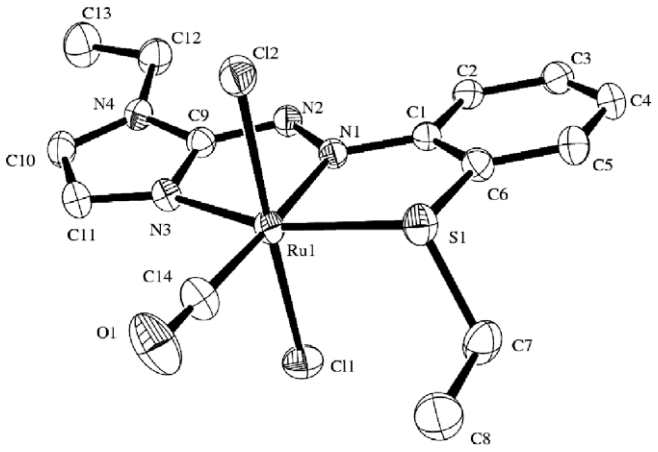


**Fig. 2.** ORTEP structure of **3b** (35% probability). Hydrogen atoms have been omitted for clarity. Selected bond lengths (Å) and angles (°): Ru1–C14 1.879(2), Ru1–N1 2.0364(17), Ru1–N3 2.0607(17), Ru1–Cl1 2.3908(9), Ru1–Cl2 2.3984(9), O1–C14 1.127(3), N1–N2 1.286(2), N1–Ru1–N3 76.65(7), S1–Ru1–N1 84.43(5), Cl1–Ru1–Cl2 176.38(2).

consequence of back bonding has been reflected in the shortening of Ru–N(azo) distance [Ru(1)–N(1), 2.0364(17) Å] compare to Ru–N(imidazole) [Ru(1)–N(3), 2.0607(17) Å]. The structural identity has been proved by DFT calculation [20] using optimized structures of **2b** and **3b**. The composition of unoccupied MOs shows the partial mixing of frontier orbitals of dπ(Ru) with the vacant $\pi^*$ orbitals of CO that implies better $d\pi(Ru^{II}) \rightarrow \pi^*(N{=}N)$ back bonding (Table S3). The theoretical Ru–N bond lengths are 0.01–0.05 Å longer than that of observed one. The experimental Ru–Cl distances are reduced by 0.04–0.05 Å than the theoretical data. The Ru–S distances are also elongated in calculated structures by ~0.06 Å. The Ru–C and C–O distances are also reduced by 0.01–0.03 Å in the experimental structures compared with their calculated structures.

Three natural bond orbitals [20] are detected for each C–O bond, and one for Ru–C bond. The Ru–C bond orbitals are polarized towards the carbon atom, and the C–O bond orbitals are polarized towards the oxygen. The occupancies and hybridization of the CO and Ru–C bonds are summarized in Supplementary Table S2. The highly populated anti-bonding NBOs (0.312–0.335) indicate the higher extent of back-donation from Ru(II) to $\pi^*$ orbitals of CO. The calculated electron population on 4d orbitals of Ru are 7.54 and 7.50 for complex **2a** and **3b,** respectively, indicates +II oxidation state of central Ru atom. The charge excess over the formal $d^6$ configuration of low spin Ru(II) arises from charge transfer from ligands. The formal charge of Ru atom is 0.014 and 0.098 in **2a** and **3b**, respectively, which are much lower than +2. The average charge on the carbon atom of the carbonyl ligands is positive (+0.639 to +0.682), while oxygen atom is negative (−0.415 to −0.440). The average charge on Cl are −0.484, and −0.502 in **2a** and **3b,** respectively. The charge on coordinated N atoms are also negative (−0.174 to −0.192, $N_{azo}$ and −0.453 to −0.492, $N_{imi}$) (Table S2).

The electronic structures of the complexes show high degree of mixing between Ru(dπ) and ligand-π and pπ of Cl. The HOMO of **2a** have 42% Ru(dπ) and 53% Cl(pπ) contribution while in **3b**, 56% Ru(dπ) and 37% Cl(pπ) contribution. HOMO-1 also caries mixture of Ru(dπ) and Cl(pπ) characters. The lowest unoccupied molecular orbital, LUMO carries >80% ligand character (L). The CO also contributes to the construction of unoccupied MOs (Table S3). The HOMO–LUMO energy gaps for the complexes are 2.32 eV (**2a**) and 1.93 eV (**3b**).

The electronic spectra of **2a**/**2b** in $CH_2Cl_2$ show an intense band at 506–510 nm corresponding to HOMO/HOMO-1 → LUMO transitions (Table 1). These are not at all pure MLCT rather admixture of MLCT and XLCT transitions (Fig. 3) (XLCT: chloride to ligand charge transfer). The complexes show two low energy bands at 790–810 and 590–595 nm which are attributed to mixed MLCT and XLCT transitions as predicted by TD DFT calculation. Intense ligand-centered bands are observed at 370–420 nm which are L(π)/Cl(pπ) → L($\pi^*$), ILCT/XLCT origin.

The complexes (**2** and **3**) show one quasireversible oxidation couple when scanned in the potential range 0.0–2.0 V vs. SCE (Fig. S2) [21] and is assigned to Ru(III)/Ru(II) redox couple as HOMO has 42% and 56% Ru(dπ) character in complex **2a** and **3b**, respectively. The Ru(III)/Ru(II) redox potential of **3a**/**3b** (0.76–0.78 V) is lower than **2a**/**2b** (1.22–1.26 V) as expected from their HOMO's energies [$E_{HOMO}$ = −5.69 eV (**2a**), −5.23 eV (**3b**)]. The complexes show three successive reduction couples in the potential range 0.0 to −2.0 V (Scheme 2). The reductions are ligand centered since LUMO, LUMO+1, LUMO+2 predominantly have ligand characteristics. Both azo (–N=N–) and imine (–C=N–) functions will be reduced accommodating electrons in the LUMOs. Two reductions

**Table 1**
Most important singlet–singlet excitations for the absorption of **2a** and **3b** in $CH_2Cl_2$ at the B3LYP/SDD level.

| Complex | Excitations | $E$ (eV) | $\lambda$ (nm) | $f$ | Character | $\lambda_{exp}$ (nm) ($\varepsilon$, $M^{-1}$ $cm^{-1}$) |
|---|---|---|---|---|---|---|
| **2a** | (72%) HOMO → LUMO | 2.2243 | 557 | 0.036 | Ru(dπ)/Cl(pπ) → N=N($\pi^*$), (MLCT, XLCT) | 506(3822) |
| | (62%) HOMO-1 → LUMO | 2.2327 | 555 | 0.0 97 | Ru(dπ)/Cl(pπ) → N=N($\pi^*$), (MLCT, XLCT) | |
| | (81%) HOMO-2 → LUMO | 2.4088 | 515 | 0.035 | S(pπ) → N=N($\pi^*$), (ILCT) | |
| | (49%) HOMO-3 → LUMO | 2.8513 | 435 | 0.145 | Cl(pπ) → N=N($\pi^*$), (XLCT) | 410(9565) |
| | (33%) HOMO-4 → LUMO | | | | | |
| | (52%) HOMO-2 → LUMO+1 | 3.0720 | 404 | 0.064 | S(pπ) → L($\pi^*$), (ILCT) | |
| | (18%) HOMO-4 → LUMO | | | | Cl(pπ) → N=N($\pi^*$), (XLCT) | |
| | (38%) HOMO-4 → LUMO | 3.1163 | 398 | 0.154 | Cl(pπ) → N=N($\pi^*$), (XLCT) | 380(8384) |
| | (26%) HOMO-2 → LUMO+1 | | | | S(pπ) → L($\pi^*$), (ILCT) | |
| **3b** | (94%) HOMO → LUMO | 1.5103 | 821 | 0.003 | Ru(dπ)/Cl(pπ) → N=N($\pi^*$), (MLCT, XLCT) | 810(921) |
| | (87%) HOMO-1 → LUMO | 2.0538 | 604 | 0.032 | Ru(dπ)/Cl(pπ) → N=N($\pi^*$), (MLCT, XLCT) | 595(2265) |
| | (47%) HOMO-2 → LUMO | 3.0135 | 411 | 0.272 | Ru(dπ)/Cl(pπ) → N=N($\pi^*$), (MLCT, XLCT) | |
| | (23%) HOMO-4 → LUMO | | | | Cl(pπ)/L(π) → N=N($\pi^*$), (XLCT, ILCT) | |
| | (48%) HOMO-5 → LUMO | 3.0865 | 402 | 0.033 | Ru(dπ)/L(π) → N=N($\pi^*$), (MLCT, ILCT) | 420(14923) |
| | (38%) HOMO-4 → LUMO | | | | Cl(pπ)/L(π) → N=N($\pi^*$), (XLCT, ILCT) | |
| | (40%) HOMO-5 → LUMO | 3.2486 | 382 | 0.072 | Ru(dπ)/L(π) → N=N($\pi^*$), (MLCT, ILCT) | |
| | (27%) HOMO-6 → LUMO | | | | Cl(pπ) → N=N($\pi^*$), (XLCT) | |
| | (92%) HOMO-7 → LUMO | 3.6683 | 338 | 0.078 | Cl(pπ)/L(π) → N=N($\pi^*$), (XLCT, ILCT) | 320(3827) |
| | (87%) HOMO-8 → LUMO | 3.8578 | 321 | 0.037 | Cl(pπ)/L(π) → N=N($\pi^*$), (XLCT, ILCT) | |

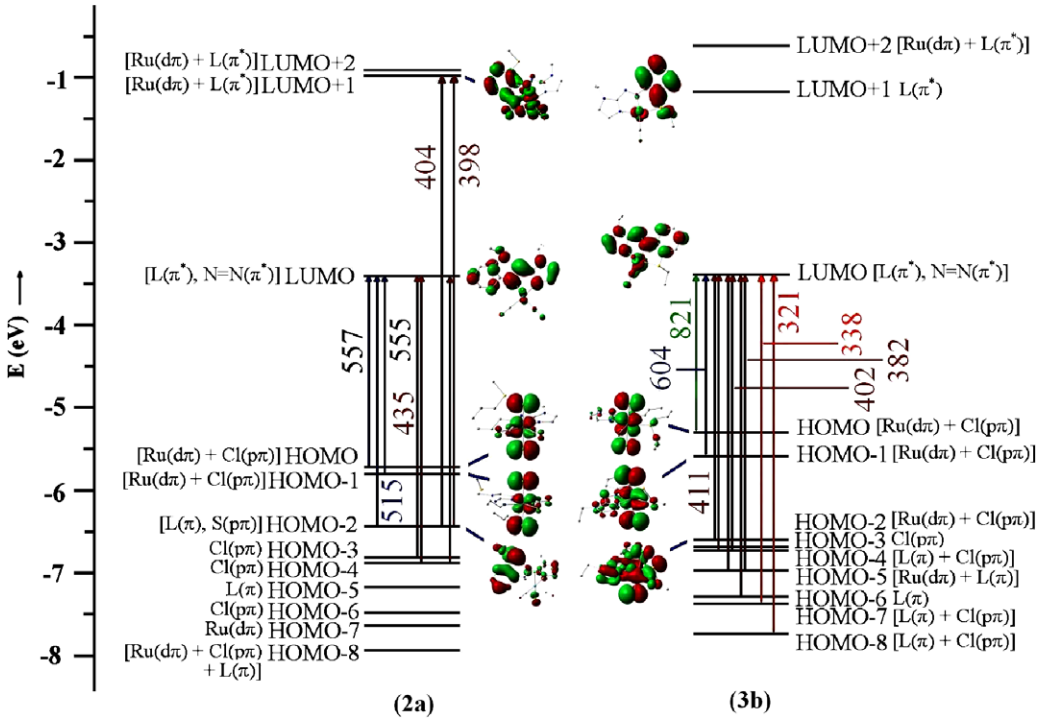


**Fig. 3.** Energy level diagrams of the molecular orbitals involved in the spin allowed singlet–singlet transitions for complexes **2a** and **3b** calculated by TDDFT in $CH_2Cl_2$ at the B3LYP/SDD level. Calculated transition energies are expressed in wavelength (nm).

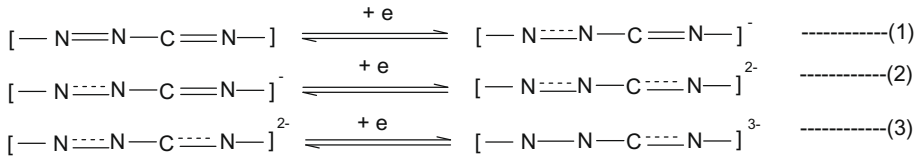


**Scheme 2.**

may be referred to azo/azo$^-$ (Eq. 1) and azo$^-$/azo = (Eq. 2) while third reduction is referred to electron insertion into –C═N– group (Eq. 3).

In conclusion, depending on hardness of central Ru(II) the ligand (L) acts as either tridentate N, N′, S or bidentate N, N′ chelator. All the complexes show low energy metal ligand to ligand charge transfer (MLLCT) band in addition to ILCT. The character of transitions has been predicted from TDDFT calculation. The complexes show one quasireversible Ru(III)/Ru(II) redox couple while three successive reductions couple of redox non-innocent ligand(L).

## Acknowledgements

Financial support from the Department of Science and Technology and University Grants Commission under CAS Scheme, New Delhi are gratefully acknowledged.

## Appendix A. Supplementary material

CCDC 673713 and 673711 contain the supplementary crystallographic data for **2a** and **3b**. These data can be obtained free of charge from The Cambridge Crystallographic Data Centre via www.ccdc.cam.ac.uk/data_request/cif.

Supplementary data associated with this article can be found, in the online version, at doi:10.1016/j.inoche.2009.12.001.

## References

[1] (a) K. Kalyansundaram, M. Gratzel, Coord. Chem. Rev. 177 (1998) 347;
(b) M.D. Ward, Chem. Soc. Rev. 24 (1995) 121;
(c) W.T. Wong, Coord. Chem. Rev. 131 (1994) 45;
(d) P.A. Anderson, R.F. Anderson, M. Furue, P.C. Junk, R.F. Keene, B.T. Patterson, B.D. Yeomens, Inorg. Chem. 39 (2000) 2721.
[2] (a) W. Kaim, S. Kohlmann, Inorg. Chem. 25 (1986) 3442;
(b) W. Kaim, S. Kohlmann, Inorg. Chem. 26 (1987) 68;
(c) M.N. Ackermann, C.R. Barton, C.J. Deodene, E.M. Specht, S.C. Keill, W.E. Schreiber, H. Kim, Inorg. Chem. 28 (1989) 397;
(d) N. Bag, A. Pramanik, G.K. Lahiri, A. Chakravorty, Inorg. Chem. 31 (1992) 40;
(e) E.Y. Li, Y.-M. Cheng, C.-C. Hsu, P.-T. Chou, G.-S. Lee, I.-H. Lin, Y. Chi, C.-S. Liu, Inorg. Chem. 45 (2006) 8041.
[3] (a) K. Kalyansundaram, Coord. Chem. Rev. 46 (1982) 159;
(b) S. Serroni, S. Campagna, F. Puntoriero, C.D. Pietro, N.D. McClenaghan, F. Loisean, Chem. Soc. Rev. 30 (2001) 367.
[4] (a) A. Dogan, B. Sarkar, A. Klein, F. Lissner, T. Schleid, J. Fiedler, S. Zalis, V.K. Jain, W. Kaim, Inorg. Chem. 43 (2004) 5973;
(b) S.J. Dougan, M. Melchart, A. Habtemariam, S. Parsons, P.J. Sadler, Inorg. Chem. 45 (2006) 10882.
[5] (a) B.K. Panda, S. Sengupta, A. Chakravorty, J. Organomet. Chem. 689 (2004) 1780;
(b) M. Panda, C. Das, G.-H. Lee, S.-M. Peng, S. Goswami, Dalton Trans. (2004) 2655;
(c) M. Panda, S. Das, G. Mostafa, A. Castineiras, S. Goswami, Dalton Trans. (2005) 1249;
(d) P. Banerjee, S. Kar, A. Bhaumik, G.-H. Lee, S.-M. Peng, S. Goswami, Eur. J. Inorg. Chem. (2007) 835;
(e) U.S. Ray, B.K. Ghosh, M. Monfort, J. Ribas, G. Mostafa, T.-H. Lu, C. Sinha, Eur. J. Inorg. Chem. (2004) 250.
[6] (a) B.G. Chand, U.S. Ray, J. Cheng, T.-H. Lu, C. Sinha, Polyhedron 22 (2003) 1213;

(b) B.G. Chand, U.S. Ray, G. Mostafa, T.-H. Lu, C. Sinha, Polyhedron 23 (2004) 1669.
[7] E. Ambundo, L.A. Ochrymowycz, D.B. Rorabacher, Inorg. Chem. 40 (2001) 5133.
[8] U.S. Ray, D. Banerjee, G. Mostafa, T.-H. Lu, C. Sinha, New J. Chem. 28 (2004) 1432.
[9] D. Banerjee, U.S. Ray, S.K. Jasimuddin, J.-C. Liou, T.-H. Lu, C. Sinha, Polyhedron 25 (2006) 1299.
[10] Synthesis of *cis*-(CO)-*trans*-(Cl)-[Ru(SMeaaiNMe)$(CO)_2Cl_2$](2a): $[Ru(CO)_2(Cl)_2]_n$ (0.31 g, 1.4 mmol) was dissolved in hot ethanol (30 ml). An ethanolic solution of SMeaaiNMe (**1a**) (0.35 g, 1.5 mmol) was added and refluxed for 2 h under $N_2$ atmosphere. The solution was cooled to room temperature. Under slow evaporation of the solvent brown crystalline product was left. The product was recrystallized from $CH_2Cl_2$–MeOH solution. The yield was 0.36 g (62%). Microanalytical data: Calc. (found). For $C_{13}H_{12}N_4O_2Cl_2Ru$ (**2a**): C, 36.45(36.36); H, 2.80(2.79); N, 13.08(13.05). $IR_{exp}$ (KBr) ($cm^{-1}$): ν(*cis*-CO) 2066, 2004, ν(C=N) 1547, ν(N=N) 1373, ν(Ru–Cl) 342. $IR_{theo}$ (b3lyp/sdd) ($cm^{-1}$): ν(CO) 2023, 2072, ν(C=N) 1575, ν(N=N) 1407, ν(Ru–Cl) 331. $E_{1/2}(Ru^{II}/Ru^{III})$, V ($\Delta E_p$, mV): 1.26(120); $E_{1/2}$ (L), V ($\Delta E_p$, mV): −0.45(80), −1.00(100), −1.44(150). The compound **2b** was prepared following the same procedure as **2a**. The yield was 65%. Microanalytical data: Calc. (found), for $C_{15}H_{16}N_4O_2Cl_2Ru$ (**2b**): C, 39.47(39.42); H, 3.51(3.51); N, 12.28(12.26). $IR_{exp}$ (KBr) ($cm^{-1}$): ν(*cis*-CO) 2062, 1998, ν(C=N) 1544, ν(N=N) 1377, ν(Ru–Cl) 341. $E_{1/2}(Ru^{II}/Ru^{III})$, V ($\Delta E_p$, mV): 1.22(120); $E_{1/2}$ (L), V ($\Delta E_p$, mV): −0.44(80), −0.98(100), −1.38(150).
[11] Synthesis of *trans*-(Cl)-[Ru(SMeaaiNMe)$(CO)Cl_2$] (**3a**); A 0.5 g (2.26 mmol) of $[Ru(CO)_2Cl_2]_n$ and 0.58 g (2.5 mmol) of SMeaaiNMe were dissolved in 40 mL acetonitrile. Freshly sublimed $Me_3NO$ (0.07 g) was added under dry $N_2$ environment. The solution was then refluxed for 3 h. The bright brown solution changed to green. Under slow evaporation of the solvent a dark green crystalline product was left. It was then dried and chromatographed and a dark green band was eluted by $C_6H_6$-acetonitrile (5:1, v/v) and evaporated in air. The yield was 0.66 g (68%). Microanalytical data: Calc. (found). For $C_{12}H_{12}N_4OCl_2Ru$ (**3a**): C, 36.00(35.92); H, 3.00(2.99); N, 14.00(13.98). $IR_{exp}$ (KBr) ($cm^{-1}$): ν(*cis*-CO) 1995, ν(C=N) 1553, ν(N=N) 1391, ν(Ru–Cl) 343. $E_{1/2}(Ru^{II}/Ru^{III})$, V ($\Delta E_p$, mV): 0.78(105); $E_{1/2}$ (L), V ($\Delta E_p$, mV): −0.48(90), −1.10(115), −1.46(140). The complex **3b** was prepared following the same procedure as **3a**. The yield was 69%. Microanalytical data: Calc. (found), for $C_{14}H_{16}N_4O_2Cl_2Ru$ (**3b**): C, 39.25(39.12); H, 3.74(3.72); N, 13.08(13.05). $IR_{exp}$ (KBr) ($cm^{-1}$): ν(*cis*-CO) 1991, ν(C=N) 1555, ν(N=N) 1396, ν(Ru–Cl) 340. $IR_{theo}$ (b3lyp/sdd) ($cm^{-1}$): ν(CO) 2015, ν(C=N) 1566, ν(N=N) 1400, ν(Ru–Cl) 324. $E_{1/2}(Ru^{II}/Ru^{III})$, V ($\Delta E_p$, mV): 0.76(105); $E_{1/2}$ (L), V ($\Delta E_p$, mV): −0.49(90), −1.12(110), −1.48(140).
[12] M.M. Khodaei, K. Bahrami, A. Karimi, Synthesis (2008) 1682;
M. Mba, L.J. Prins, G. Licini, Org. Lett. 9 (2007) 21.
[13] K.K. Sarker, B.G. Chand, K. Suwa, J. Cheng, T.-H. Lu, J. Otsuki, C. Sinha, Inorg. Chem. 46 (2007) 670;
K.K. Sarker, d. Sardar, K. Suwa, J. Otsuki, C. Sinha, Inorg. Chem. 46 (2007) 8291;
P. Pratihar, T.K. Mondal, A.K. Patra, C. Sinha, Inorg. Chem. 48 (2009) 2760.
[14] T. Yutaka, M. Kurihara, .H. Nishihara, Mol. Cryst. Liquid Cryst. 343 (2000) 193;
T. Yutaka, L. Mori, M. Kurihara, J. Mizutani, K. kubo, S. Furusho, K. Matsumura, N. Tamai, H. Nishihara, Inorg. Chem. 40 (2001) 4986.
[15] Single crystal data collections were performed with an automated Bruker SMART APEX CCD diffractometer. Unit cell parameters were determined from least-squares refinement of setting angles ($\theta$) within the range $1.45 \leqslant \theta \leqslant 25.98°$ (**2a**) and $2.00 \leqslant \theta \leqslant 28.09°$ (**3b**). Out of 5797 collected data 3241 for **2a**, and 14823 collected data 4090 for **3b** with $I > 2\sigma(I)$ were used for structure solution. The *hkl* ranges are $-9 \leqslant h \leqslant 9$, $-10 \leqslant k \leqslant 10$, $-17 \leqslant l \leqslant 17$ for **2a**, and $-13 \leqslant h \leqslant 13$, $-14 \leqslant k \leqslant 14$, $-20 \leqslant l \leqslant 20$ for **3b**. Reflection data were recorded using the $\omega$ scan technique. Data were corrected for Lorentz polarization effects and for linear decay. Semi-empirical absorption corrections based on $\psi$-scans were applied. The structure were solved by direct method using SHELXS-97 [G. M. Sheldrick, SHELXS-97, University of Gottingen, Germany, 1997] and successive difference Fourier syntheses. All non-hydrogen atoms were refined anisotropically. The hydrogen atoms were fixed geometrically and refined using the riding model. All calculation were carried out using SHELXL-97 [G.M. Sheldrick, SHELXL 97, University of Gottingen, Germany, 1997], ORTEP-32 [L.J. Farrugia, ORTEP-3 for windows, J. Appl. Cryst. 30 (1997) 565], and PLATON-99 [A.L. Spek, PLATON, The Netherlands, 1999] programs.
[16] (a) B.K. Ghosh, A. Chakravorty, Coord. Chem. Rev. 95 (1989) 239;
(b) T.K. Misra, D. Das, C. Sinha, P.K. Ghosh, C.K. Pal, Inorg. Chem. 37 (1998) 1672;
(c) S. Serroni, S. Campagna, F. Puntoriero, C.D. Pietro, N.D. Mcclenaghan, F. Loiseau, Chem. Soc. Rev. 30 (2001) 367;
(d) P. Byabartta, J. Dinda, P.K. Santra, C. Sinha, K. Panneerselvam, F.-L. Liao, T.-H. Lu, J. Chem. Soc., Dalton Trans. (2001) 2825;
(e) R.E. Shepherd, Coord. Chem. Rev. 247 (2003) 147;
(f) S. Patra, B. Sarkar, S. Maji, J. Fiedler, F.A. Urbanos, R. Jimenez-Aparicio, W. Kaim, G.K. Lahiri, Chem. – A: Eur. J. 12 (2006) 489.
[17] (a) T.K. Mondal, J.-S. Wub, T.-H. Lu, S.K. Jasimuddin, C. Sinha, J. Organomet. Chem. 694 (2009) 3518;
(b) T.K. Mondal, S.K. Sarker, P. Raghavaiah, C. Sinha, Polyhedron 27 (2008) 3020.
[18] J.E. Huheey, E.A. Keiter, R.L. Keiter, Inorganic Chemistry Harper Collins, fourth ed., Addison-Wesley Publishing Company, 2000.
[19] J. Otsuki, K. Suwa, K. Narutaki, C. Sinha, I. Yoshikawa, K. Araki, J. Phys. Chem. A 109 (2005) 8064;
P. Bhunia, B. Baruri, U.S. Ray, C. Sinha, S. Das, J. Cheng, T.-H. Lu, Transit. Met. Chem. 31 (2006) 310.
[20] Full geometry optimizations were carried out using the density functional theory method at the (R)B3LYP level for **2a** and **3b** [C. Lee, W. Yang, R.G. Parr, Phys. Rev. B 37 (1988) 785]. Elements except ruthenium were assigned a 6-311G(d) basis set in these calculation. The SDD basis set with effective core potential was employed for ruthenium atom [P. Fuentealba, H. Preuss, H. Stoll, L.V. Szentpaly, Chem. Phys. Lett. 89 (1989) 418]. All calculation were performed with Gaussian03 program package [M.J. Frisch et al., Gaussian 03, Revision D.01, Gaussian Inc., Wallingford CT, 2004] with the aid of the GaussView visualization program. Natural bond orbital analyses were performed using the NBO 3.1 module of Gaussian03 [NBO Version 3.1, E.D. Glenening, A.E. Reed, J.E. Carpenter, F. Weinhold]. Vertical electronic excitations based on B3LYP optimized geometries was computed using the time-dependent density functional theory (TDDFT) formalism [R. Bauernschmitt, R. Ahlrichs, Chem. Phys. Lett. 256 (1996) 454] in dichloromethane using conductor-like polarizable continuum model (CPCM) [V. Barone, M. Cossi, J. Phys. Chem. A 102 (1998) 1995]. GaussSum [N.M. O'Boyle, A.L. Tenderholt, K.M. Langner, J. Comput. Chem. 29 (2008) 839] was used to calculate the fractional contributions of various groups to each molecular orbital.
[21] Electrochemical measurements were performed using computer-controlled PAR model 250 VersaStat electrochemical instruments with Pt-disk milli working electrode, Pt-auxiliary and SCE as reference. All measurements were carried out under nitrogen environment at 298 K in acetonitrile using $[nBu_4N][ClO_4]$ as supporting electrolyte at 50 mV $S^{-1}$ scan rate.